Chitinase 3-like 1 is a profibrogenic factor overexpressed in the aging liver and in patients with liver cirrhosis

Norihisa Nishimura[a], Davide De Battista[a], David R. McGivern[b], Ronald E. Engle[a], Ashley Tice[a], Rafaelle Fares-Gusmao[b], Juraj Kabat[c], Anna Pomerenke[a], Hanh Nguyen[a], Shinya Sato[a], Kevin W. Bock[d], Ian N. Moore[d], David E. Kleiner[e], Fausto Zamboni[f], Harvey J. Alter[g,1], Sugantha Govindarajan[h], and Patrizia Farci[a,1]

[a]Hepatic Pathogenesis Section, Laboratory of Infectious Diseases, National Institute of Allergy and Infectious Diseases, NIH, Bethesda, MD 20892; [b]Center for Biologics Evaluation and Research, US Food and Drug Administration, Silver Spring, MD 20993; [c]Biological Imaging Facility Research Technologies Branch, National Institute of Allergy and Infectious Diseases, NIH, Bethesda, MD 20892; [d]Infectious Disease Pathogenesis Section, National Institute of Allergy and Infectious Diseases, NIH, Bethesda, MD 20892; [e]Laboratory of Pathology, National Cancer Institute, NIH, Bethesda, MD 20892; [f]Liver Transplantation Center, Azienda Ospedaliera Brotzu, 09134 Cagliari, Italy; [g]Department of Transfusion Medicine, Clinical Center, NIH, Bethesda, MD 20892; and [h]Department of Pathology, Rancho Los Amigos Hospital, University of Southern California, Los Angeles, CA 90242

Contributed by Harvey J. Alter, March 3, 2021 (sent for review September 30, 2020; reviewed by Meena B. Bansal and Andrea Cox)

Older age at the time of infection with hepatitis viruses is associated with an increased risk of liver fibrosis progression. We hypothesized that the pace of fibrosis progression may reflect changes in gene expression within the aging liver. We compared gene expression in liver specimens from 54 adult donors without evidence of fibrosis, including 36 over 40 y old and 18 between 18 and 40 y old. *Chitinase 3-like 1* (*CHI3L1*), which encodes chitinase-like protein YKL-40/CHI3L1, was identified as the gene with the greatest age-dependent increase in expression in liver tissue. We investigated the cellular source of CHI3L1 in the liver and its function using liver tissue specimens and in vitro models. *CHI3L1* expression was significantly higher in livers of patients with cirrhosis of diverse etiologies compared with controls represented by patients who underwent liver resection for hemangioma. The highest intrahepatic *CHI3L1* expression was observed in cirrhosis due to hepatitis D virus, followed by hepatitis C virus, hepatitis B virus, and alcohol-induced cirrhosis. In situ hybridization of *CHI3L1* messenger RNA (mRNA) identified hepatocytes as the major producers of CHI3L1 in normal liver and in cirrhotic tissue, wherein hepatocytes adjacent to fibrous septa showed higher *CHI3L1* expression than did those in more distal areas. In vitro studies showed that recombinant CHI3L1 promotes proliferation and activation of primary human hepatic stellate cells (HSCs), the major drivers of liver fibrosis. These findings collectively demonstrate that CHI3L1 promotes liver fibrogenesis through a direct effect on HSCs and support a role for CHI3L1 in the increased susceptibility of aging livers to fibrosis progression.

CHI3L1 | aging | liver fibrosis | cirrhosis

It is well-established that the incidence of severe liver disease with rapid liver fibrosis progression in humans is increased in the elderly, although the underlying mechanisms remain to be elucidated (1). The role of age has been particularly well documented in patients with hepatitis C virus (HCV) infection, where age at the onset of infection was found to be a major determinant for fibrosis progression and disease severity in immunocompetent subjects (2–6). Likewise, donor age was shown to have a major impact on graft outcome after liver transplantation for end-stage HCV disease: When the donors were younger than 40, the interval to cirrhosis was 10 y, whereas when the donors were 41 to 50 or older, the intervals were 6.7 and 2.7 y, respectively (7). Collectively, these data suggest that age-related changes in liver response to injury play a key role in determining the increased susceptibility of the aging liver to fibrosis (2, 4, 7).

We hypothesized that the different rate of liver fibrosis progression in patients over 40 y of age could reflect changes in gene expression in aging livers. To test this hypothesis, we studied a large series of liver specimens from 54 well-characterized liver transplant donors by comparing gene expression between liver donors less than and over 40 y of age. We identified *chitinase 3-like 1* (*CHI3L1*) as the gene with the greatest age-dependent increase in expression. CHI3L1, also known as YKL-40 in humans, is a secreted glycoprotein of ∼40 kDa (8), which has been shown to play a critical role in a variety of human diseases associated with inflammation, tissue remodeling, and injury (9–12). A correlation between serum levels of CHI3L1 with aging was previously documented in a large cohort of healthy individuals in Denmark (13). Elevated levels of CHI3L1 in serum have also been reported as a biomarker of liver fibrosis in patients with chronic liver disease of any etiology (9, 12, 14–18). However, the mechanisms underlying the correlation between increased circulating CHI3L1 levels and liver fibrosis have not yet been determined. There is very limited information on the expression of *CHI3L1* in primary liver tissue, since in most previous studies serum was the sole clinical material analyzed. Thus, in this study, we investigated the source of CHI3L1 and the mechanisms linking CHI3L1 with liver fibrosis by using primary liver tissue and in vitro models.

Significance

Older age at the time of hepatitis virus infection and age of liver donors are major determinants of liver fibrosis progression and disease severity. Our study demonstrates that aging is accompanied by significant changes in gene expression and identifies a gene, *chitinase 3-like 1* (*CHI3L1*), as having the greatest age-dependent increase in expression and as being overexpressed in cirrhotic livers. Our in vivo and in vitro results provide evidence that CHI3L1 plays a central role in liver fibrogenesis and support a role for CHI3L1 in the increased susceptibility of aging livers to fibrosis progression. This study may open avenues for specific antifibrotic or microRNA therapy to reduce or prevent hepatic fibrosis and its ominous complications.

Author contributions: N.N., F.Z., and P.F. designed research; N.N., D.D.B., D.R.M., R.E.E., A.T., R.F.-G., A.P., H.N., S.S., K.W.B., I.N.M., D.E.K., S.G., and P.F. performed research; N.N., D.D.B., J.K., D.E.K., F.Z., H.J.A., S.G., and P.F. analyzed data; and N.N., D.D.B., D.R.M., R.E.E., H.J.A., and P.F. wrote the paper.

Reviewers: M.B.B., Mount Sinai School of Medicine; and A.C., Johns Hopkins University School of Medicine.

The authors declare no competing interest.

[1]To whom correspondence may be addressed. Email: halter@dtm.cc.nih.gov or patrizia.farci@nih.gov.

This article contains supporting information online at https://www.pnas.org/lookup/suppl/doi:10.1073/pnas.2019633118/-/DCSupplemental.

Published April 22, 2021.

Results

Characteristics of the Normal Liver Donors. A total of 54 liver donors were included in this study. The demographic characteristics and the results of hepatitis serology and liver histology of these subjects are presented in *SI Appendix*, Table S1. They were divided into two groups according to their age: The first group included 18 subjects aged 40 y or less (mean, 27.9; range, 19 to 40) that we defined as younger donors, and the second group included 36 subjects over 40 y old (mean, 57.5; range, 42 to 75) that we defined as older donors. Male donors were predominant in both groups with 11 of 18 (61%) in the younger and 21 of 36 (58%) in the older group. None of the liver specimens obtained from the 54 donors included in this study had histological evidence of liver fibrosis; one donor in the younger group and six in the older group showed minimal to mild steatosis.

Gene Expression Profiling of Liver Donors Identifies CHI3L1 as the Most Up-Regulated Gene in Aging Livers. To identify genes that are differentially regulated in the aging liver, we performed transcriptomics analysis in each of the 54 liver specimens obtained from organ donors who had normal liver without evidence of hepatic fibrosis. Comparison of the genes between older and younger donors identified 13 genes that were differentially expressed with a P value <0.001 (Fig. 1*A* and *SI Appendix*, Table S2). Among these genes, seven were up-regulated (*CHI3L1*, *ZIC1*, *TBX15*, *LGALS4*, *CSTA*, *ERICH5*, *KDSR*) and six were down-regulated (*SERPINI1*, *SSBP2*, *KCNJ3*, *RBMS1*, *ZNF518B*, *AIF1L*) in the livers of older donors (Fig. 1*A*). A heatmap of these 13 genes showed a clear separation between older and younger liver donors (Fig. 1*B*). Since gene expression profiling was performed in histologically normal liver specimens, these data indicate that age, independent of histology, affects the expression of liver genes. Gene Ontology analysis showed that the differentially expressed genes in older donors are involved in fibrogenesis, tumor suppression, DNA damage, and cell-cycle regulation (*SI Appendix*, Table S3). Among the up-regulated genes detected in older donors, we found that *CHI3L1* was the most up-regulated with the highest fold change. This finding was of particular significance because elevated serum CHI3L1 levels were previously reported in a large body of literature as a biomarker for staging liver fibrosis in patients with chronic hepatitis of any etiology (9, 14–19) and CHI3L1 was shown to play a critical role in lung and kidney fibrogenesis (20, 21, 15). Our liver microarray data confirm observations in serum from healthy individuals (13), which showed that CHI3L1 levels increase with age. Details on the other genes that were differentially expressed in older liver donors are provided in *SI Appendix*, *Results*.

Expression of *CHI3L1* in Liver Tissue of Organ Donors. To investigate the cellular localization and expression of *CHI3L1* in the liver, we performed in situ hybridization (ISH) in formalin-fixed and paraffin-embedded (FFPE) liver sections obtained from 20 donors (including 10 donors older than 40 y and 10 donors younger than 40 y) using sequence-specific probes. As an internal control and to identify hepatocytes, sections were costained for albumin (*ALB*) messenger RNA (mRNA), which was highly expressed in hepatocytes from donors in both age groups. The livers studied had normal histology with no signs of liver fibrosis (Fig. 1*C*). By ISH, we found that *CHI3L1* mRNA was primarily expressed in hepatocytes (*ALB*+ cells) and was more abundant in tissue from older donors compared with younger donors (Fig. 1*D*). *CHI3L1* mRNA levels in tissue sections correlated with microarray data, being more highly expressed in older than younger liver donors. Additional evidence that hepatocytes are a major source of CHI3L1 in the liver was obtained by analyzing *CHI3L1* expression in the liver of four patients with hepatitis B virus (HBV)-associated acute liver failure that we recently studied (22), whose liver pathology showed massive liver necrosis and infiltration of a large number of inflammatory cells (*SI Appendix*, Fig. S1*A*). By quantitative reverse-transcription polymerase chain reaction (qRT-PCR), we found that intrahepatic *CHI3L1* was almost undetectable in all four patients (*SI Appendix*, Fig. S1*B*), further confirming that hepatocytes are a major source of CHI3L1 in the liver.

FFPE liver specimens obtained from 52 liver donors were available for CHI3L1 staining, including 36 subjects older than 40 and 16 younger than 40 y. In line with the increased *CHI3L1* mRNA levels observed by microarray and by ISH in aging livers, we found that the levels of the CHI3L1 protein in liver tissue were remarkably higher in the cytoplasm of hepatocytes in older donors, where positive staining was observed in all liver donors (Fig. 1*E*), thus confirming the microarray data. In contrast, younger donors showed negative staining in three donors (18.7%), with the majority (77%) showing weak or very weak reactivity. Only one young liver donor showed strong cytoplasmic staining. Thus, these data were consistent with the significantly higher expression of *CHI3L1* both at mRNA levels detected by microarray and ISH and protein levels in the older group compared with the younger group.

Expression of CHI3L1 in Patients with Chronic Liver Diseases. Although elevated serum CHI3L1 has been proposed as a biomarker of liver fibrosis, there is very limited information on the expression of *CHI3L1* in the fibrotic liver, which is the anatomical site of the disease. To further elucidate the biological and clinical significance of circulating CHI3L1, we investigated the expression of *CHI3L1* mRNA by performing qRT-PCR in liver specimens from a cohort of 64 well-characterized patients with cirrhosis of different etiology. The demographic, clinical, histopathological, and virological features are reported in Table 1. The majority were males; patients with alcoholic cirrhosis were the youngest, followed by those with HCV cirrhosis. A history of excessive alcohol consumption was also reported in 50% of HCV patients. The lowest alanine aminotransferase and aspartate aminotransferase values were seen in alcoholic cirrhosis, whereas the highest values were seen in HCV cirrhosis (Table 1). There were no significant differences in γ-glutamyltransferase among the four groups. Patients with hepatitis D virus (HDV) cirrhosis showed the lowest platelet counts, consistent with the typical splenomegaly associated with HDV disease (23), and the highest activity grade as compared with alcoholic, HCV-, and HBV-associated diseases ($P < 0.001$), confirming that HDV is the most severe form of chronic viral hepatitis (Table 1). In this cohort of patients, all had cirrhosis (97%) with the exception of two cases in the HBV hepatocellular carcinoma (HCC) group. HCV replication was detected in all patients with HCV cirrhosis with a mean of 4.7 logs IU/mL. Interestingly, we did not see any difference in *CHI3L1* expression in HCV cirrhotic patients infected with different HCV genotypes, both in liver and in serum (*SI Appendix*, Fig. S2). HBV DNA replication levels were very low in HBV and HDV, with a mean log of 2.0 ± 0.5 and 1.4 ± 0.3 IU/mL, respectively. Serum HDV RNA was positive in all patients with HDV cirrhosis, along with immunoglobulin G (IgG) anti-HD and immunoglobulin M (IgM) anti-HD in 82% of them.

CHI3L1 mRNA was detected in each of the cirrhotic liver specimens analyzed. The median levels of intrahepatic *CHI3L1* expression were significantly higher in all groups of cirrhotic patients than the levels in controls (Fig. 2*A*). Patients with HDV cirrhosis showed the highest median level, which was significantly higher than the levels in alcoholic cirrhosis, HCV cirrhosis, and nontumorous HBV HCC. In patients with end-stage liver disease there is a loss of vast areas of hepatic parenchyma, which is replaced by wide bands of fibrotic tissue devoid of hepatocytes (*SI Appendix*, Fig. S1 *C–F*). The intrahepatic CHI3L1 levels were elevated in all patients with end-stage cirrhosis, in particular in HDV cirrhosis (Fig. 2*A*). The liver *CHI3L1* expression correlated with the circulating CHI3L1 levels (Fig. 2*B*), which were significantly higher than the levels in controls. Consistent with the liver expression, the highest serum values were seen in HDV cirrhosis. A significant correlation between liver and serum levels was found among all groups studied (Fig. 2*C*).

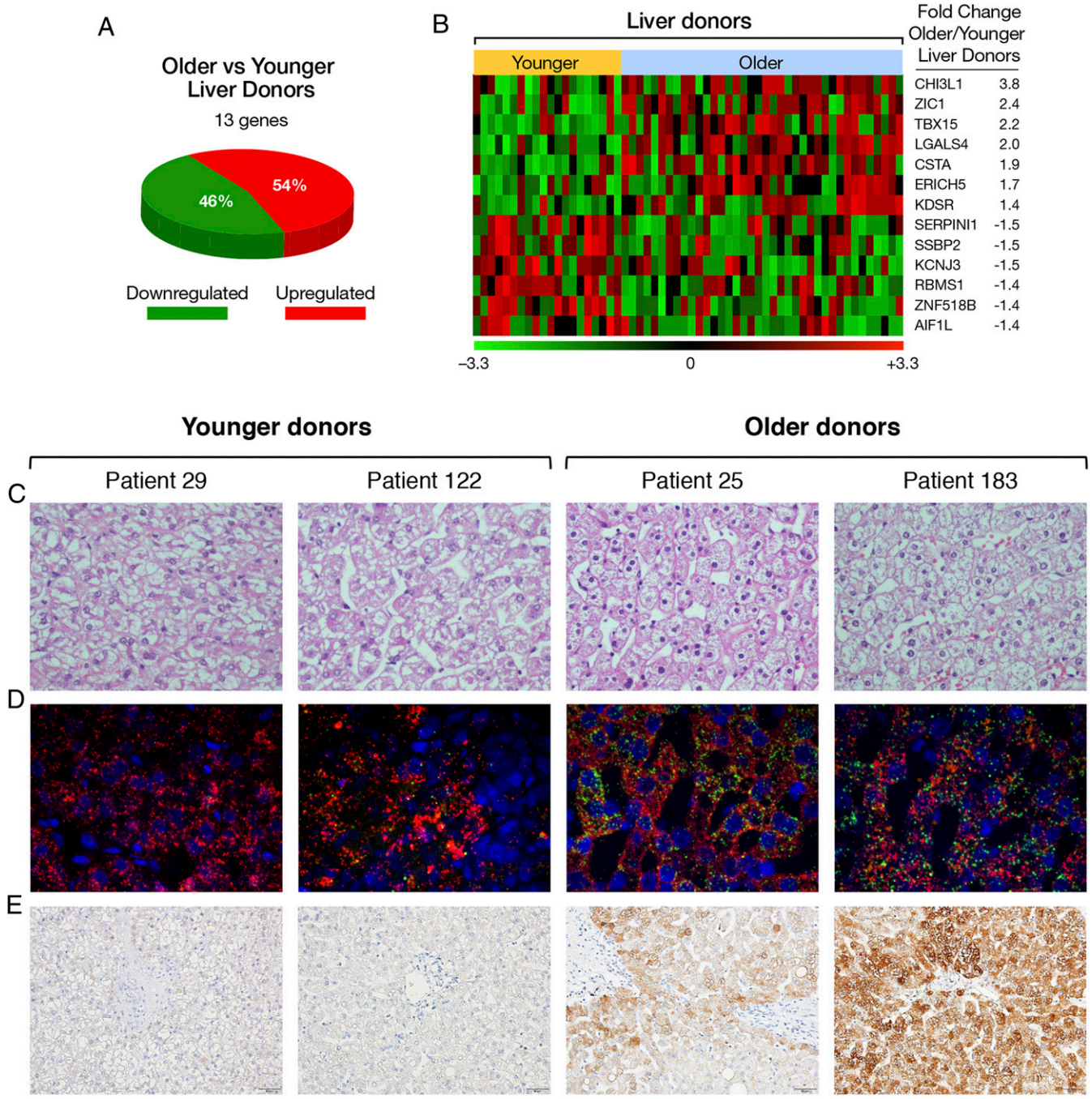

Fig. 1. Gene expression profiling, in situ hybridization, and immunolocalization of CHI3L1 in liver specimens from younger and older liver donors. Comparison between older and younger liver donors identified 13 genes that were differentially expressed ($P < 0.001$) with a fold change higher than 1.4. (*A*) Pie chart indicating the number of up- and down-regulated genes identified in the liver of donors older than 40 y of age. (*B*) Heatmap showing the differential expression of the 13 genes in younger and older donors. Fold changes were calculated as the ratio between older and younger liver donors. Positive and negative fold changes represent genes that were found to be up- and down-regulated, respectively, in older liver donors. Each row represents data for a specific human gene, and each column represents the expression of genes in a single liver specimen. Gene expression levels were $\log_2$-transformed. The color in each cell reflects the level of expression of the corresponding gene in the corresponding liver specimen. Up-regulated genes are shown in shades of red and down-regulated genes are in shades of green. (*C*) Hematoxylin and eosin staining in paraffin sections obtained from liver tissue of four representative subjects, including two younger (40 y of age or less) and two older (more than 40 y) liver donors, all exhibiting normal liver histology and absence of hepatic fibrosis, is shown. (*D*) Representative confocal microscopic images (40× magnification) of in situ hybridization for *CHI3L1* mRNA (green) and *ALB* mRNA (red) in FFPE sections obtained from liver tissue of four representative cases, including two younger and two older liver donors. Tissues were counterstained with DAPI to visualize nuclei. (*E*) Representative images of immunohistochemical staining for CHI3L1 in paraffin sections from liver tissues of the same four representative cases described above, showing higher CHI3L1 expression in older liver donors (20× magnification).

The expression of *CHI3L1* mRNA was also investigated by ISH in the liver from two patients with HCV cirrhosis and two with HDV cirrhosis. *CHI3L1* was abundant and expressed at high levels in hepatocytes, which also coexpressed *ALB* mRNA (Fig. 2*D*), whereas *CHI3L1* mRNA was not observed in the *ALB*-negative nonhepatocyte cells within the fibrous septa (Fig. 2 *E*–*G*).

Table 1. Demographic, clinical, serological, and histopathological characteristics of 64 patients with chronic liver disease of different etiology

	Etiologic diagnosis			
	Alcoholic	HCV	HBV	HDV
Demographic and clinical characteristics				
Patients, no.	16	25	12	11
Age, y	52.3 ± 1.5*	48.4 ± 1.3†	58.6 ± 2.4	56.6 ± 1.5
Male, no. (%)	13 (81.3)	25 (100.0)	11 (91.7)	8 (72.7)
Alanine aminotransferase, U/L‡	32.1 ± 3.8§	97.0 ± 14.8¶	42.2 ± 7.9	73.2 ± 15.2
Aspartate aminotransferase, U/L#	47.8 ± 3.8‖	170.8 ± 33.3**	44.5 ± 6.9	81.9 ± 12.4
γ-Glutamyltransferase, U/L††	41.9 ± 5.7	79.2 ± 15.1	88.6 ± 24.5	81.7 ± 15.9
Platelets, $10^3/\mu L$‡‡	92 ± 9.7§§	80 ± 6.7	147 ± 27¶¶	65 ± 9.2
Liver pathology				
Cirrhosis, no.	16	25	10	7
HCC-nontumorous tissue, no.	0	0	12	4
Activity grade	4.3 ± 0.3##	6.5 ± 0.5	5.0 ± 0.5	10.5 ± 1.1***
Fibrosis stage	6.0 ± 0.0	6.0 ± 0.0	5.5 ± 0.3	6.0 ± 0.0
Hepatitis serology				
HBsAg-positive, no. (%)	0	0	12 (100)	11 (100)
Anti-HBs–positive, no. (%)	7 (37)	9 (36)	0	0
Anti-HBc–positive, no. (%)	6 (37)	11 (44)	12 (100)	11 (100)
Anti-HBe–positive, no. (%)	NT	NT	12 (100)	11 (100)
Serum HBV DNA, $\log_{10}$, IU/mL	0	0	2.0 ± 0.5	1.4 ± 0.3
Anti-HCV–positive, no. (%)	1 (6)	25 (100)	0	1 (1)
Serum HCV RNA, $\log_{10}$, IU/mL	0	4.7 ± 0.2	0	0
HCV genotype	NA		NA	NA
1a/1b		7		
Non-1		17		
Anti-HD IgG-positive, no. (%)	0	0	0	11 (100)
Anti-HD IgM-positive, no. (%)	0	0	0	9 (82)
Serum HDV RNA-positive, no. (%)	0	0	0	11 (100)

Plus–minus values are means ± SEM. HCV, denotes hepatitis C virus; HBV, hepatitis B virus; HDV, hepatitis D virus; NT, not tested; NA, not applicable.
*$P = 0.003$ for the comparison with HBV.
†$P = 0.041$ for the comparison with HBV.
‡Normal range ≤43 UI/L.
§$P = 0.0015$ for the comparison with HCV.
¶$P = 0.021$ for the comparison with HBV.
#Normal range ≤42 UI/L.
‖$P = 0.003$ for the comparison with HCV.
**$P = 0.006$ for the comparison with HBV.
††Normal range ≤38 UI/L.
‡‡Normal range ≥ 159 to ≤388 $10^3/\mu L$.
§§$P = 0.027$ for the comparison with HBV.
¶¶$P = 0.002$ for the comparison with HDV and HCV.
##$P = 0.041$ for the comparison with HCV.
***$P \leq 0.0001$ for the comparison with alcoholic cirrhosis, HCV cirrhosis, and nontumorous HBV; all statistical comparisons were done using the Tukey test.

Notably, in contrast to the uniform distribution detected in liver donors throughout the lobule, *CHI3L1* expression was not evenly distributed within the cirrhotic livers. In both HDV (Fig. 2 *D–F*) and HCV cirrhosis (Fig. 2*G*), higher *CHI3L1* mRNA levels were observed in hepatocytes adjacent to fibrous septa or in hepatocytes trapped within fibrous septa (Fig. 2*F*), whereas *CHI3L1* was not detected within the fibrous septa. The lack of *CHI3L1* expression in fibrous septa was also confirmed by immunohistochemistry in both HCV and HDV cirrhosis (*SI Appendix*, Fig. S3). An example of the spatial distribution of CHI3L1 in the cirrhotic liver is shown in a representative patient infected with HDV (*SI Appendix*, Fig. S4).

CHI3L1 Is Produced by Primary Human Hepatocytes and Activated Primary Hepatic Stellate Cells In Vitro. To further confirm that hepatocytes express *CHI3L1*, we studied in vitro cultured primary human hepatocytes obtained from liver donors. Analysis by qRT-PCR demonstrated that *CHI3L1* is constitutively expressed by primary human hepatocytes, while it is not expressed by hepatocellular carcinoma cell lines (HepG2 and Huh7) (Fig. 3*A*). CHI3L1 appears to be retained within hepatocytes as the amount of CHI3L1 in the culture supernatant was very low (Fig. 3*B*). Additional evidence was obtained by confocal microscopy (Fig. 3*C*), which showed the presence of CHI3L1 within the cytoplasm of cultured primary human hepatocytes.

As serum levels of CHI3L1 were reported as a biomarker that may predict the stage of liver fibrosis in patients with chronic hepatitis (14–16), we hypothesized that CHI3L1 could also be produced by hepatic stellate cells (HSCs), the most important effector cells in driving liver fibrogenesis (24). To test this hypothesis, we cultured isolated primary human HSCs and tested the expression of *CHI3L1* mRNA in the cell lysates and culture supernatants collected at different time points (days 2, 4, 6, and 8). Little, if any, expression of *CHI3L1* was detected at day 2; however, starting at day 4, the expression of *CHI3L1* increased over time in parallel with the release of

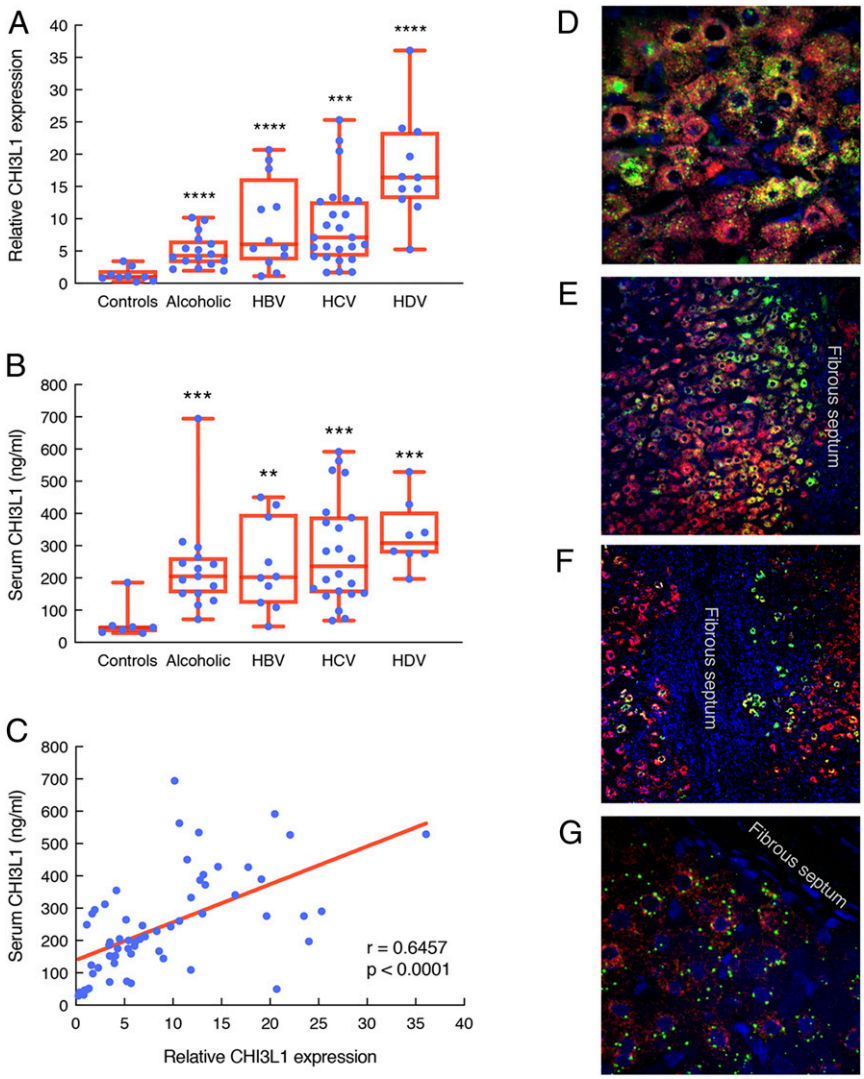

Fig. 2. Increased levels of liver and circulating CHI3L1 in patients with liver cirrhosis of different etiology. (*A* and *B*) Levels of *CHI3L1* expression in liver (*A*) and serum (*B*) of patients with alcoholic cirrhosis, HBV cirrhosis, HCV cirrhosis, HDV cirrhosis, and controls. The median of the values for each patient group is indicated by a horizontal line in each box, with the 25th and 75th percentiles indicated at the top and bottom of each box; the 10th and 90th percentiles are indicated at the top and bottom of each I bar. Significance was determined using the Mann–Whitney *U* test for the comparison between each type of cirrhosis and the control group. $^{**}P < 0.01$, $^{***}P < 0.001$, $^{****}P < 0.0001$. (*C*) Correlation between liver and circulating CHI3L1 was determined in all groups studied using Spearman's rank-correlation coefficient. (*D*–*G*) Confocal microscopic images of in situ hybridization for *CHI3L1* mRNA (green) and *ALB* mRNA (red) in FFPE sections obtained from liver tissue of one representative patient with HDV cirrhosis (*D*–*F*) and one with HCV cirrhosis (*G*) showing the boundary between the liver parenchyma and a fibrous septum (*E*–*G*); 40× magnification (*D* and *G*); 10× magnification (*E* and *F*).

CHI3L1 protein levels in the supernatant of primary HSCs (Fig. 3 *D* and *E*). This rise in *CHI3L1* expression was paralleled by an increased expression of HSC activation markers, including alpha-smooth muscle actin 2 (*ACTA2*), collagen type 1 alpha 1 (*COL1A1*), and transforming growth factor beta 1 (*TGF-β1*) (Fig. 3 *G*–*I*). Taken together, these data indicate that not only hepatocytes but also HSCs can be a source of CHI3L1, supporting the role of CHI3L1 in fibrogenesis. Additional proof that human HSCs produce CHI3L1 was obtained by qRT-PCR (*SI Appendix*, Fig. S5*A*), Western blot analysis (*SI Appendix*, Fig. S5*B*), and confocal microscopy, which documented the presence of CHI3L1 in HSCs with a cytoplasmic distribution (*SI Appendix*, Fig. S5*C*). In contrast, we found that the cell line LX2 generated by immortalization of primary human HSCs does not produce CHI3L1, as documented by qRT-PCR, Western blot, and confocal microscopy (*SI Appendix*, Figs. S5 *A*, *B*, and *D*). Thus, the synthesis of CHI3L1 is a feature restricted to primary hepatocytes and activated primary human HSCs, while it was not detected in immortalized cell lines like Huh7, HepG2, and LX2.

CHI3L1 Promotes Hepatic Stellate Cell Proliferation and Activation. To elucidate the role of CHI3L1 in liver fibrogenesis, we investigated the effect of recombinant human CHI3L1 (rhCHI3L1) on the proliferative response of primary human HSCs and compared the results with those obtained with unstimulated cells. First, we performed a serial twofold titration curve to investigate the dose–response effect of rhCHI3L1 on HSC proliferation starting from 500 ng, which was the dose used in previous reports (25, 26). The results showed a significant effect of rhCHI3L1 in the dose range between 62.5 and 500 ng/mL, as compared with unstimulated cells (*SI Appendix*, Fig. S6*A*). As a positive control, cells were stimulated with recombinant human platelet-derived growth factor BB (rhPDGF-BB), the most potent inducer of HSC proliferation (27). We found that the rate of HSC proliferation was significantly higher

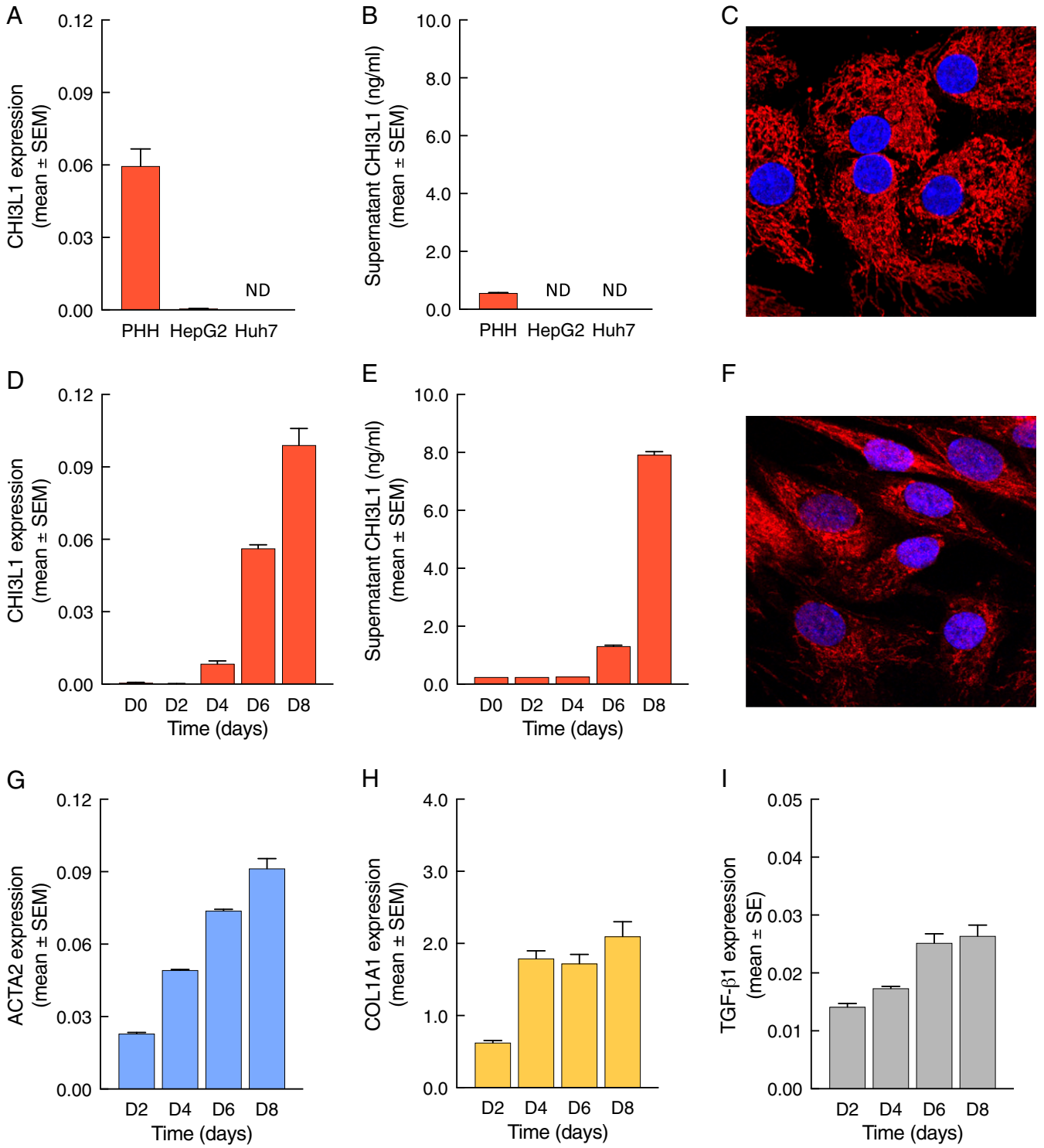

Fig. 3. Hepatocytes and hepatic stellate cells are a source of CHI3L1. (*A* and *B*) Expression of *CHI3L1* in cultured primary human hepatocytes (PHH) and in the hepatoma cell lines HepG2 and Huh7 as measured by qRT-PCR in cell lysates (*A*) and by enzyme-linked immunosorbent assay (ELISA) in supernatants (*B*) from primary human hepatocytes and HepG2 and Huh7 cells. (*C*) Representative confocal microscopic image of primary human hepatocytes stained for CHI3L1 (red). (*D* and *E*) Expression of *CHI3L1* in activated primary human hepatic stellate cells as measured by qRT-PCR in cell lysates (*D*) and by ELISA in supernatants (*E*) from primary human hepatic stellate cells. (*F*) Confocal microscopic image of primary human hepatic stellate cells stained for CHI3L1 (red); 63× magnification. (*G–I*) Markers of hepatic stellate cell activation, including *ACTA2* (*G*), *COL1A1* (*H*), and *TGF-β1* (*I*), were measured by qRT-PCR in primary human hepatic stellate cells at the indicated times after plating. Results are the average of two independent experiments; each sample was run in duplicate (*A*, *B*, *D*, *E*, and *G–I*). Values represent means ± SEM. ND, not detectable.

in cells treated with rhCHI3L1 compared with unstimulated cells using both 500 (Fig. 4*A*) and 62.5 ng/mL (*SI Appendix*, Fig. S6*B*), whereas no significant difference was observed between cells treated with rhCHI3L1 versus rhPDGF-BB. These results were also confirmed by immunofluorescence staining for Ki67, which is a specific marker of proliferating cells (28). The percentage of

Ki67 nuclear positivity was significantly higher in cells stimulated with rhCHI3L1 or rhPDGF-BB than in untreated cells (Fig. 4*B* and *SI Appendix*, Fig. S6*C*). Altogether, these data indicate that CHI3L1 possesses mitogenic properties.

To evaluate whether CHI3L1 also induces activation of HSCs, we performed qRT-PCR of cell lysates at different time points until day 8. We found that stimulation with rhCHI3L1 significantly increased the expression of *ACTA2* and *COL1A1* (Fig. 4 *C* and *D*) but not of *TGF-β1* (Fig. 4*E*), compared with untreated cells, suggesting that the profibrogenic effect of CHI3L1 in promoting HSC activation is independent of TGF-β1 signaling. In response to liver injury, cross-talk occurs between inflammatory cells and activated HSCs. Thus, we also investigated the effect of several human recombinant cytokines, including recombinant human interleukin-6 (rhIL-6), recombinant human C-C motif chemokine ligand 2 (rhCCL2), rhTNF-α, rhTGF-β1, and rhIL-13 on *CHI3L1* expression, in both primary human hepatocytes and HSCs. Only treatment with rhIL-6 significantly increased the expression of *CHI3L1* in primary hepatocytes (Fig. 5*A*), but not in primary human HSCs (Fig. 5*B*), whereas only TNF-α significantly increased *CHI3L1* expression in HSCs but not in primary hepatocytes (Fig. 5 *A* and *C*). By contrast, all the other cytokines showed no effect (Fig. 5 *D*–*F*).

Discussion

Our study provides evidence that aging is accompanied by significant changes in gene expression in the liver and identifies *CHI3L1* as the most up-regulated gene in liver donors over 40 y of age. This increase was seen in histologically normal livers with no signs of fibrosis, demonstrating that the increase in liver *CHI3L1* expression occurs during the normal aging process. Correlation of CHI3L1 with aging was previously documented in healthy individuals, in which the levels of circulating CHI3L1 were found to increase exponentially with age (13). The mechanisms underlying age-dependent increases in *CHI3L1* expression and the role of age-related CHI3L1 elevation in liver fibrosis progression remain unknown. One potential mechanism is altered gene expression due to age-dependent epigenetic alterations. DNA methylation levels at specific loci across human tissues have been shown to correlate with chronological age (29). These age-dependent epigenetic changes in DNA methylation are known to impact gene expression and contribute to age-related disease (30, 31). However, the specific impact of epigenetic changes on *CHI3L1* expression has not been characterized. Previous studies have shown that elevated circulating CHI3L1 levels correlate with the degree of liver fibrosis in patients with chronic hepatitis B and C, alcoholic liver disease, and nonalcoholic steatohepatitis (14–17, 19, 32, 33). However, in most of these studies, serum was the only clinical material analyzed and therefore the cellular source of circulating CHI3L1 was not defined, nor was the relationship between CHI3L1 and liver fibrosis evaluated.

An important feature of our experimental approach is the use of paired liver and serum samples from a large cohort of patients with liver cirrhosis of different etiology to study *CHI3L1* expression. We found that the expression of *CHI3L1* is significantly increased in all forms of cirrhosis, from alcoholic to type B, C, and D cirrhosis, compared with controls. Our data also show that in patients with HCV cirrhosis the HCV genotype does not influence the expression of *CHI3L1*, including HCV genotype 3, which has been associated with an accelerated progression to cirrhosis (34).

The highest expression of *CHI3L1* in the liver was found in cirrhosis caused by HDV, a highly pathogenic virus that causes the least common but most severe and rapidly progressive form of chronic viral hepatitis (23). Notably, despite the dependence of HDV on HBV (35), the levels of CHI3L1 were significantly higher in HDV than in HBV cirrhosis, which suggests that CHI3L1 levels may influence the rate of fibrosis progression. Our study also showed that *CHI3L1* expression levels in the liver positively correlated with CHI3L1 levels in circulation. However, differences in circulating levels did not reach statistical significance among the different forms of cirrhosis. This may be due to the fact that circulating CHI3L1 levels do not solely reflect the expression in the liver. Indeed, a variety of cells produce CHI3L1, including macrophages, neutrophils, chondrocytes, fibroblasts, endothelial cells, airway epithelial cells, and other cells, all of which may contribute to CHI3L1 elevations in serum in human diseases characterized by acute or chronic inflammation and tissue remodeling (12).

Analysis of *CHI3L1* mRNA distribution by ISH in liver donors and cirrhotic livers confirmed that hepatocytes are the major producers of CHI3L1 and showed a difference in the spatial distribution of this protein between normal and cirrhotic livers. In normal livers, *CHI3L1* mRNA was evenly distributed throughout the parenchyma within the lobule. In cirrhotic livers, as we documented in type D and C cirrhosis, the spatial distribution of *CHI3L1* mRNA follows a gradient with the highest expression in hepatocytes adjacent to the fibrous septa, while *CHI3L1* mRNA was not detectable in the cells within the fibrous septa. The lack of CHI3L1 in fibrous septa of patients with end-stage liver cirrhosis, detected by ISH and immunohistochemistry, suggests that the production of CHI3L1 in vivo may change during the progression of liver fibrosis. While in the early phase of liver injury, CHI3L1 release by hepatocytes may activate HSCs that, in turn, produce CHI3L1 through an autocrine loop, in the late phase of advanced liver fibrosis, activated HSCs are differentiated into myofibroblasts that produce fibrillary type 1 collagen and express alpha-SMA (36) but not CHI3L1, as shown by our data. In contrast, hepatocytes remain a major source of CHI3L1 in the liver throughout the progression of liver fibrosis, leading to cirrhosis and end-stage liver disease, as shown by the strong expression of *CHI3L1* that we documented in hepatocytes both at the level of mRNA by ISH and protein by immunohistochemistry. Consistent with our in vivo data, *CHI3L1* mRNA was not detected in the liver of patients who developed HBV-associated acute liver failure (22), characterized by a massive loss of hepatocytes. Taken together, our data provide compelling evidence that hepatocytes are the major source of CHI3L1 in the liver and that the levels of this protein are significantly elevated in patients with cirrhosis.

Although CHI3L1 is known to be a biomarker of liver fibrosis, whether it plays a direct role in the pathogenesis of liver fibrosis remains to be established. Since HSCs are the major effectors in liver fibrogenesis (37), we used primary human HSCs as an in vitro model to investigate the underlying mechanisms linking CHI3L1 with liver fibrosis. Following liver injury or in vitro culture, HSCs become activated and transdifferentiate from a nonproliferative quiescent phenotype into proliferative, fibrogenic myofibroblasts (24, 38, 39). Our work provides evidence that activated primary human HSCs are another important source of CHI3L1 in addition to hepatocytes and that CHI3L1 directly promotes fibrogenic activity in primary HSCs. We found that treatment with rhCHI3L1 alone is sufficient to stimulate HSC proliferation with a trend that did not differ significantly from that induced by rhPDGF-BB (Fig. 4), one of the most potent mitogens for HSCs (27). In addition, our in vitro study demonstrates that the effect of CHI3L1 extends beyond proliferation, as this protein stimulates the production of COL1A1 and ACTA2, two key markers of HSC activation (24, 38). The production of COL1A1 by recombinant CHI3L1 was comparable to that induced by TGF-β1. However, stimulation with TGF-β1 did not result in an increased expression of *CHI3L1*, suggesting that CHI3L1 production is regulated independent from TGF-β1, as previously shown for IL-13–induced activation of fibrogenesis (40). Our in vitro data indicate that CHI3L1 exerts major biological functions on HSCs. It shares the potent mitogenic effect of PDGF while behaving like TGF-β1 for the production of extracellular matrix, type 1 collagen. Our in vitro data were obtained with primary HSCs isolated from

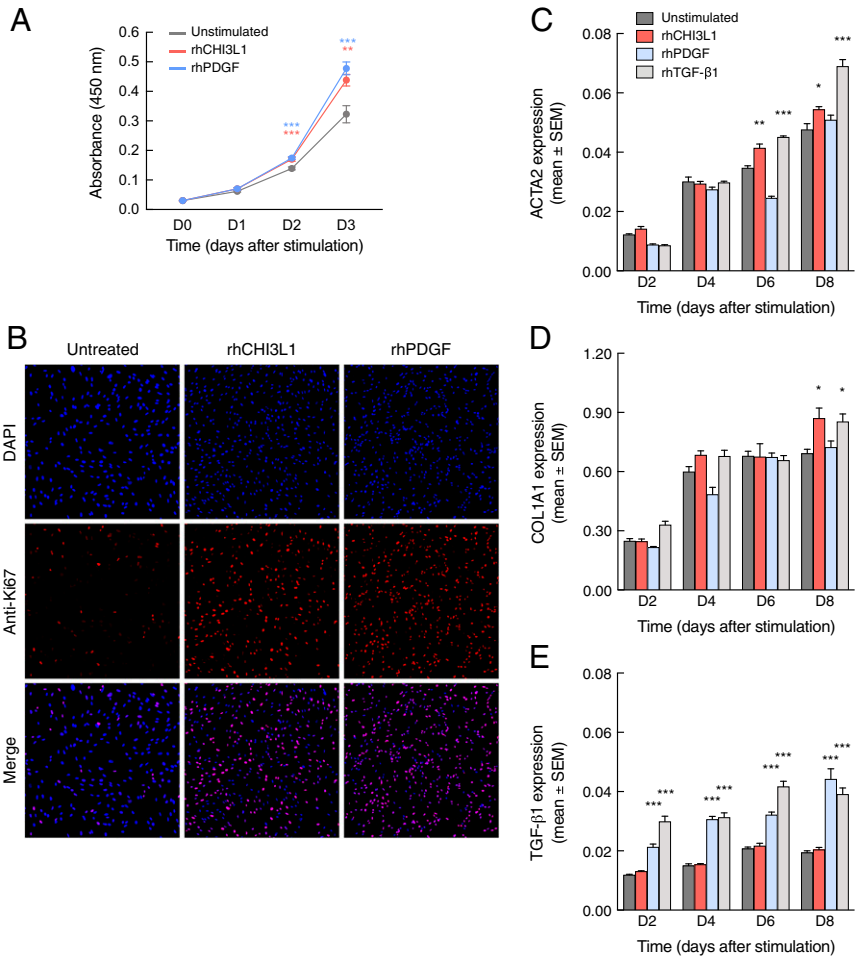

Fig. 4. Recombinant human CHI3L1 promotes proliferation and activation of primary human hepatic stellate cells in vitro. (*A*) Proliferation of primary human hepatic stellate cells treated with rhCHI3L1 or rhPDGF-BB or unstimulated. Cellular proliferation was measured by CCK8 assay. rhCHI3L1 significantly increased the proliferation rate of hepatic stellate cells compared with unstimulated cells. The stimulatory effect of rhCHI3L1 was similar to that observed with rhPDGF-BB after both 48 and 72 h of stimulation. Results are the average of three independent experiments, in which six replicate wells were used for each condition at each time point. Values represent means ± SEM. (*B*) Immunofluorescence staining for the proliferation marker Ki67 in primary human hepatic stellate cells treated with either rhCHI3L1 or rhPDGF-BB or unstimulated as analyzed by confocal microscopy (4 × 4 tiles acquired with a 63× objective) at high magnification (7× zoom). The percentage of Ki67-positive cells was significantly higher in cultures treated with rhCHI3L1 than in unstimulated cells. The proliferative effect of rhCHI3L1 was similar to that seen in cultures treated with rhPDGF-BB. Expression of genes associated with hepatic stellate cell activation was measured by qRT-PCR in primary hepatic stellate cells treated with rhCHI3L1 (500 ng/mL), rhPDGF-BB (20 ng/mL), or rhTGF-β1 (10 ng/mL) or unstimulated. (*C–E*) Expression of *ACTA2* (*C*), *COL1A1* (*D*), and *TGF-β1* (*E*) is shown. Results are the average of two independent experiments; each sample was run in duplicate. Values represent means ± SEM. Significance was determined using unpaired Student's *t* test for the comparison between each type of stimulation and the unstimulated control at the respective time point. **P* < 0.05, ***P* < 0.01, ****P* < 0.001.

livers without fibrosis and followed for up to 8 d in culture. In contrast, our in vivo studies were performed in patients with established cirrhosis and end-stage liver disease, with wide bands of fibrotic tissue and the presence of myofibroblasts, which produce collagen and express alpha-SMA. The difference between these two settings may explain the lack of CHI3L1 within fibrous septa. Further studies are necessary to investigate the expression of *CHI3L1* in activated HSCs in different stages of liver fibrosis, especially during the early phase before advanced fibrosis is established.

Inflammation is the major force driving liver fibrosis (41). Proliferation of HSCs at the site of injury is typically preceded by an influx of inflammatory cells, including Kupffer cells, other macrophages, and immune cells, all of which produce inflammatory cytokines (38). Thus, we investigated the role of different cytokines in regulating the expression of *CHI3L1*. We found that the proinflammatory cytokine IL-6 significantly increased the expression of *CHI3L1* in primary hepatocytes, but not HSCs, whereas TNF-α was associated with a significant increase in *CHI3L1* expression in primary HSCs, but not hepatocytes. In contrast, we did not observe any effect on *CHI3L1* expression when either cell type was stimulated with CCL2, IL-13, or TGF-β1, further confirming that the stimulation of CHI3L1 production is independent of TGF-β1. Our data are consistent with the hypothesis that, if older individuals undergo liver injury, necrosis of the hepatocytes may release their CHI3L1 content, whose quantity significantly increases in aging livers as we have documented in this study. This may represent an important stimulus for HSC proliferation and activation, which in turn may lead to further release of CHI3L1 contributing to the perpetuation of HSC activation and the magnification of inflammatory infiltrates. When the liver injury persists, this creates the best environment for CHI3L1 to act as a critical early mediator of liver fibrogenesis through an autocrine loop enacted by HSCs, which both produce

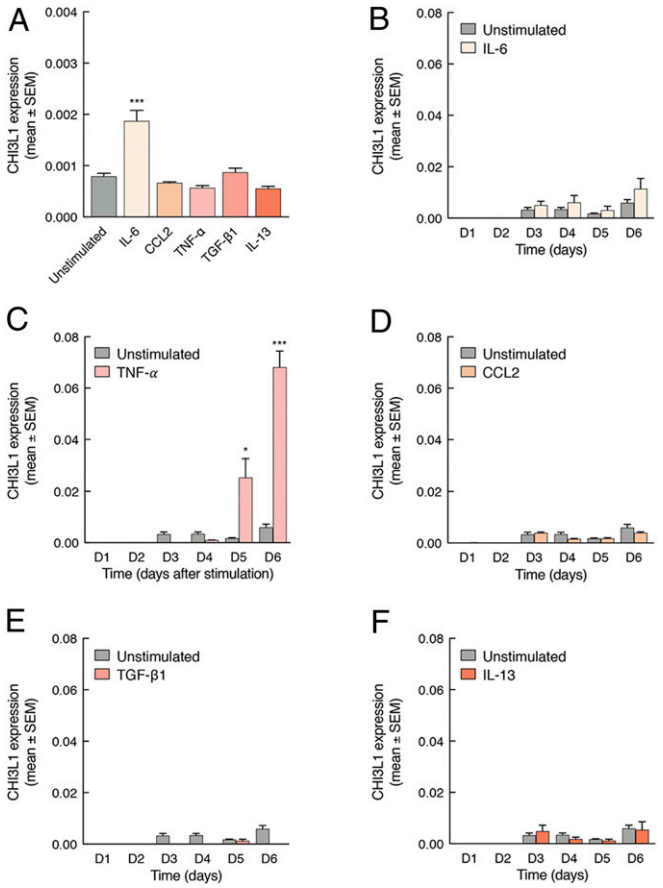

Fig. 5. Effect of stimulation of primary human hepatocytes and primary human hepatic stellate cells with different cytokines on *CHI3L1* expression. (*A*) *CHI3L1* expression, as measured by qRT-PCR, 48 h after stimulation of primary human hepatocytes with recombinant human cytokines: rhIL-6 (50 ng/mL), rhCCL2 (50 ng/mL), rhTNF-α (50 ng/mL), rhTGF-β1 (10 ng/mL), and rhIL-13 (20 ng/mL). Results are the average of three independent experiments; each sample was run in duplicate. Values represent means ± SEM. (*B–F*) *CHI3L1* expression, as measured by qRT-PCR, at different time points after stimulation of primary human hepatic stellate cells with rhIL-6 (50 ng/mL) (*B*), rhTNF-α (50 ng/mL) (*C*), rhCCL2 (50 ng/mL) (*D*), rhTGF-β1 (10 ng/mL) (*E*), and rhIL-13 (20 ng/mL) (*F*). Expression of *CHI3L1* was measured by qRT-PCR. Results are the average of two independent experiments; each sample was run in duplicate. Values represent means ± SEM. Significance was determined using unpaired Student's *t* test for the comparison between each type of stimulation and the unstimulated control at the respective time point. $*P < 0.05$, $***P < 0.001$.

and are activated by this protein. Although the clinical relevance of our in vitro data remains speculative, the substantial evidence that serum CHI3L1 is a biomarker of liver fibrosis (14–17, 32) combined with our in vivo and in vitro findings collectively support a role for CHI3L1 in liver fibrogenesis. Our work provides a mechanism to explain the link between elevated levels of CHI3L1 and liver fibrosis. In addition, the elevated levels of CHI3L1 in older individuals provide insights into the role of age in liver fibrosis.

In conclusion, our study demonstrates that the expression of *CHI3L1* is higher in older than younger liver donors and that this protein is overexpressed in the liver tissue of patients with cirrhosis, in particular HDV cirrhosis, the most rapidly progressive form of chronic viral hepatitis. Prospective studies will be required to investigate whether higher CHI3L1 levels early in the disease course may identify patients at higher risk of fibrosis progression. Taken together, our in vivo and in vitro results collectively suggest that CHI3L1 is not simply a biomarker of liver fibrosis but that CHI3L1 plays a central role in liver fibrogenesis through a direct effect on HSCs and contributes to the increased susceptibility of aging livers to fibrosis progression. A better understanding of the biological role of CHI3L1 in liver fibrogenesis may open new avenues for specific antifibrotic therapy to reduce or prevent the progression of hepatic fibrosis and, ultimately, the ominous complications of liver cirrhosis.

Materials and Methods

Study Design. We studied three cohorts of patients. The first cohort included 54 liver donors aged 18 to 75 y divided into two groups according to age; a liver specimen was obtained from each donor. This cohort included 18 liver donors aged 40 y or below and 36 over 40 y. None of the subjects included in this cohort had any history of liver disease or heavy alcohol consumption (more than 20 g/day), and all were negative for markers of infection with hepatitis B, C, or D viruses as well as other known viral infections included in the mandatory screening for liver donors. The demographic characteristics and the results of hepatitis serology and liver histology of these subjects are presented in *SI Appendix*, Table S1. Gene expression profiling, which was performed in all 54 subjects, identified CHI3L1 as the most up-regulated gene. Based on the results obtained by microarray, we studied paired serum and liver specimens from a second cohort of 64 patients with chronic liver disease including 16 with alcoholic cirrhosis, three females and 13 males, aged 52 ± 1.5 y (mean ± SEM); 25 with hepatitis C virus cirrhosis, all males, aged 48.4 ± 1.3 y; 12 patients with HBV-associated hepatocellular carcinoma, one female and 11 males, aged 56.6 ± 2.4 y; and 11 with hepatitis D virus-associated disease, three females and eight males, including seven with cirrhosis and three with cirrhosis-associated HCC, aged 56.6 ± 1.5 y. Patients underwent liver transplantation for end-stage liver disease or HCC with the exception of four with HCC who underwent partial hepatectomy at the Department of Surgery and Liver Transplantation Center of the Hospital Brotzu. In patients with associated HCC, the liver specimen was obtained in each case from the surrounding nontumorous tissue. All patients underwent mandatory screening at the time of liver transplantation for HBV, HCV, and HDV viruses. The clinical, serological, virological, and histopathological data are available for all patients (Table 1). The etiologic diagnosis of alcoholic cirrhosis was based on a history of alcohol consumption over 80 g daily for 8 y or more in the absence of markers of active infection with hepatitis viruses, including HBV, HCV, or HDV. The diagnosis of HCV cirrhosis was based on the presence of antibody to HCV and serum HCV RNA. Half of HCV patients also reported a history of excessive alcohol consumption (over 60 g daily). The HCV genotype was genotype 1a/1b in 8, and non-1 in the remaining 17; all patients were negative for serological markers of active infection with HBV and HDV. Patients with diagnosis of HBV-associated HCC were positive for hepatitis B surface antigen (HBsAg), antibody to hepatitis B core antigen (anti-HBc), and antibody to hepatitis B e antigen (anti-HBe) and negative for hepatitis B e antigen (HBeAg) and antibody to HBsAg (anti-HBs). Patients were receiving antiviral treatment with nucleos(t)ide analogs prior to liver transplantation or surgery. Patients with HDV disease were all positive for HBsAg, anti-HBc, and anti-HBe and negative for anti-HBs; serum HDV RNA was detectable in all patients along with IgG anti-HD and 82% of them were also positive for IgM anti-HD. One patient with HCC was also positive for anti-HCV but repeatedly negative for serum HCV RNA. None of the 64 patients studied was positive for antibody to HIV type 1. Patients with HBV and HDV disease were part of previous studies on gene expression profiling (42, 43). In patients with HBV-associated HCC, we analyzed only specimens obtained from the surrounding nontumorous area, from the most distant nontumorous area; each liver specimen was analyzed by an expert hepatopathologist (D.E.K. and S.G.) and liver specimens containing a mixed population of malignant and nonmalignant hepatocytes were excluded from the study. As a control group, we studied a third cohort of normal liver specimens obtained from nine individuals during surgical resection for hepatic hemangioma (mean age 49.3 ± 10 y; eight women and one man). None of them had evidence of infection with hepatitis viruses nor a history of alcohol abuse. The liver histology was normal in all. Liver specimens were obtained at the time of liver transplantation or during resection. Concomitant with the liver biopsy, one aliquot of serum was also obtained and stored at −80 °C for further analysis. The levels of CHI3L1 were quantified in serum and liver of cirrhotic patients and in the control group. To identify the cellular source and visualize the spatial distribution of *CHI3L1* expression in the liver, ISH was performed in a subgroup of 20 patients, including 10 younger and 10 older liver donors, and in four cirrhotic patients. To protect the identity of the study subjects, liver and serum specimens as well as clinical data were obtained under code. All patients provided

written informed consent, and the protocol was approved by the ethical committee of the Hospital Brotzu. The study was also approved by the Office of Human Subjects Research of the NIH, granted on the condition that all samples were deidentified.

Liver Pathology. Each liver specimen was divided into two pieces: One half was snap-frozen and stored at −80 °C for molecular studies, while the other was formalin-fixed and paraffin-embedded for pathological examination and immunohistochemistry, as previously reported (44). All liver biopsies were analyzed blindly by two expert hepatopathologists (D.E.K. and S.G.). For each liver specimen, the grade of inflammation and the stage of fibrosis were established according to the Ishak et al. scoring system (45).

Gene Expression Profiling. Gene expression profiling was performed in all 54 liver specimens obtained from transplant donors using Affymetrix Human U133 Plus 2 arrays, which represent 33,000 unique human genes (46). Total RNA was extracted using TRIzol reagent (Invitrogen) according to the manufacturer's recommendations, as previously reported (46). Quality and integrity of RNA were assessed using the RNA 6000 Nano Assay on the Agilent 2100 Bioanalyzer. Total RNA (50 ng) obtained from frozen liver tissue was subjected to two successive rounds of amplification (47); RNA labeling and hybridization were performed according to the standard Affymetrix protocols. Microarray data are available at the Gene Expression Omnibus (https://www.ncbi.nlm.nih.gov/geo) under accession no. GSE152738.

Statistical Analysis. Microarray data were analyzed using BRB-ArrayTools version 4.6.0-beta-1 (48). Microarray raw data (CEL files) were imported into BRB-ArrayTools (22). Probe set summaries were normalized using the RMA method, as previously reported (22, 43). Data from multiple microarrays from a single liver specimen were averaged. Transcripts with minimal variation across the set of arrays (less than 1.5-fold deviation from the median in more than 80% of the arrays) were not included in the analysis (43). Statistical analyses were performed using data that were $\log_2$-transformed. Fold changes were calculated as the ratio between the geometric means of older and younger liver tissue donors (43). Positive and negative fold changes represent genes that were found to be up- and down-regulated, respectively, in older liver donors, as previously described (43, 46). A total of 5,139 genes passed the filtering criteria. To identify genes that were differentially expressed, we compared the group of older liver donors with the younger group by applying a *t* test using a *P* value below 0.001 and a fold change higher than 1.4. Clustering of gene expression profiling was visualized by Partek Genomic Suite version 7.0. Pathway analysis was performed using the method of the Efron–Tibshirani gene set analysis (49), which is implemented by the BRB-ArrayTools for assessing significance of predefined gene sets. We used this method to analyze BioCarta pathways. An ANOVA was used to test for significant differences between mean values of continuous variables whenever data from all four groups of patients were analyzed; we then used the Tukey test for comparison of groups.

Visualization of *CHI3L1* mRNA in Liver Tissue by In Situ Hybridization. Sections of FFPE liver tissue specimens (5-μm thickness) from 20 liver donors including 10 younger and 10 older individuals and from seven patients with liver cirrhosis were stained for *CHI3L1* and human serum *ALB* mRNAs by ISH using the ViewRNA Tissue Assay (Invitrogen) according to the manufacturer's protocol. Probe catalog nos. VA1-3002031 and VA6-13354 were used to detect *CHI3L1* and *ALB* mRNAs, respectively. Sections were counterstained with DAPI before mounting. Images were acquired using an oil immersion 40× or 63× objective lens on a Zeiss Cell Observer SD spinning disk confocal microscope with a Yokogawa CSU-X1 scan head.

Detection of CHI3L1 in Liver Tissue by Immunohistochemistry. Details are described in *SI Appendix, Materials and Methods*.

Gene Expression Analysis of *CHI3L1* by qRT-PCR in Liver Tissue of Patients with Liver Cirrhosis and in Controls. Details are described in *SI Appendix, Materials and Methods*.

Measurement of Serum YKL-40/CHI3L1. Details are described in *SI Appendix, Materials and Methods*.

Cells and In Vitro Culture Systems, Cell Proliferation and Ki67 Staining of Primary Human HSCs, and Activation of Primary Human HSCs. Details are described in *SI Appendix, Materials and Methods*.

Gene Expression Analyses in Cell-Culture Systems. Details are described in *SI Appendix, Materials and Methods*.

Western Blot Analysis. Details are described in *SI Appendix, Materials and Methods*.

Data Availability. All data associated with this study are present in the paper or *SI Appendix*. Microarray data are available in the Gene Expression Omnibus (https://www.ncbi.nlm.nih.gov/geo) under accession no. GSE152738.

ACKNOWLEDGMENTS. This work was supported by the Intramural Research Program of the National Institute of Allergy and Infectious Diseases and the National Cancer Institute, NIH, and by intramural funds from the Center for Biologics Evaluation and Research, US Food and Drug Administration. We thank the Microscopy and Core Imaging Facility of the Center for Biologics Evaluation and Research.

1. D. L. Schmucker, Age-related changes in liver structure and function: Implications for disease? *Exp. Gerontol.* **40**, 650–659 (2005).
2. T. Poynard, P. Bedossa, P. Opolon, Natural history of liver fibrosis progression in patients with chronic hepatitis C. The OBSVIRC, METAVIR, CLINIVIR, and DOSVIRC groups. *Lancet* **349**, 825–832 (1997).
3. H. J. Alter, L. B. Seeff, Recovery, persistence, and sequelae in hepatitis C virus infection: A perspective on long-term outcome. *Semin. Liver Dis.* **20**, 17–35 (2000).
4. J. M. Hui *et al*., Insulin resistance is associated with chronic hepatitis C virus infection and fibrosis progression [corrected]. *Gastroenterology* **125**, 1695–1704 (2003).
5. S. Boccato *et al*., Fibrosis progression in initially mild chronic hepatitis C. *J. Viral Hepat.* **13**, 297–302 (2006).
6. A. Alberti, L. Chemello, L. Benvegnù, Natural history of hepatitis C. *J. Hepatol.* **31** (suppl. 1), 17–24 (1999).
7. M. Wali, R. F. Harrison, P. J. Gow, D. Mutimer, Advancing donor liver age and rapid fibrosis progression following transplantation for hepatitis C. *Gut* **51**, 248–252 (2002).
8. M. Rehli, S. W. Krause, R. Andreesen, Molecular characterization of the gene for human cartilage gp-39 (CHI3L1), a member of the chitinase protein family and marker for late stages of macrophage differentiation. *Genomics* **43**, 221–225 (1997).
9. J. S. Johansen, Studies on serum YKL-40 as a biomarker in diseases with inflammation, tissue remodelling, fibroses and cancer. *Dan. Med. Bull.* **53**, 172–209 (2006).
10. G. L. Chupp *et al*., A chitinase-like protein in the lung and circulation of patients with severe asthma. *N. Engl. J. Med.* **357**, 2016–2027 (2007).
11. L. S. Knudsen *et al*., Plasma IL-6, plasma VEGF, and serum YKL-40: Relationship with disease activity and radiographic progression in rheumatoid arthritis patients treated with infliximab and methotrexate. *Scand. J. Rheumatol.* **35**, 489–491 (2006).
12. C. G. Lee *et al*., Role of chitin and chitinase/chitinase-like proteins in inflammation, tissue remodeling, and injury. *Annu. Rev. Physiol.* **73**, 479–501 (2011).
13. S. E. Bojesen, J. S. Johansen, B. G. Nordestgaard, Plasma YKL-40 levels in healthy subjects from the general population. *Clin. Chim. Acta* **412**, 709–712 (2011).
14. C. Nøjgaard *et al*.; EMALD Group, Serum levels of YKL-40 and PIIINP as prognostic markers in patients with alcoholic liver disease. *J. Hepatol.* **39**, 179–186 (2003).
15. G. Esmat *et al*., Evaluation of serum biomarkers of fibrosis and injury in Egyptian patients with chronic hepatitis C. *J. Hepatol.* **46**, 620–627 (2007).
16. E. Kumagai *et al*., Serum YKL-40 as a marker of liver fibrosis in patients with non-alcoholic fatty liver disease. *Sci. Rep.* **6**, 35282 (2016).
17. L. Yan, Y. Deng, J. Zhou, H. Zhao, G. Wang; China HepB-Related Fibrosis Assessment Research Group, Serum YKL-40 as a biomarker for liver fibrosis in chronic hepatitis B patients with normal and mildly elevated ALT. *Infection* **46**, 385–393 (2018).
18. A. D. Kjaergaard, J. S. Johansen, S. E. Bojesen, B. G. Nordestgaard, Role of inflammatory marker YKL-40 in the diagnosis, prognosis and cause of cardiovascular and liver diseases. *Crit. Rev. Clin. Lab. Sci.* **53**, 396–408 (2016).
19. R. J. Fontana *et al*.; HALT-C Trial Group, Serum fibrosis markers are associated with liver disease progression in non-responder patients with chronic hepatitis C. *Gut* **59**, 1401–1409 (2010).
20. Y. Zhou *et al*., Chitinase 3-like 1 suppresses injury and promotes fibroproliferative responses in mammalian lung fibrosis. *Sci. Transl. Med.* **6**, 240ra76 (2014).
21. T. A. Montgomery *et al*., Breast regression protein-39/chitinase 3-like 1 promotes renal fibrosis after kidney injury via activation of myofibroblasts. *J. Am. Soc. Nephrol.* **28**, 3218–3226 (2017).
22. Z. Chen *et al*., Role of humoral immunity against hepatitis B virus core antigen in the pathogenesis of acute liver failure. *Proc. Natl. Acad. Sci. U.S.A.* **115**, E11369–E11378 (2018).
23. P. Farci, G. A. Niro, Clinical features of hepatitis D. *Semin. Liver Dis.* **32**, 228–236 (2012).
24. T. Tsuchida, S. L. Friedman, Mechanisms of hepatic stellate cell activation. *Nat. Rev. Gastroenterol. Hepatol.* **14**, 397–411 (2017).
25. C. H. He *et al*., Chitinase 3-like 1 regulates cellular and tissue responses via IL-13 receptor α2. *Cell Rep.* **4**, 830–841 (2013).
26. B. Geng *et al*., Chitinase 3-like 1-CD44 interaction promotes metastasis and epithelial-to-mesenchymal transition through β-catenin/Erk/Akt signaling in gastric cancer. *J. Exp. Clin. Cancer Res.* **37**, 208 (2018).
27. M. Pinzani *et al*., Mitogenic signals for platelet-derived growth factor isoforms in liver fat-storing cells. *Am. J. Physiol.* **260**, C485–C491 (1991).

28. L. T. Li, G. Jiang, Q. Chen, J. N. Zheng, Ki67 is a promising molecular target in the diagnosis of cancer (review). *Mol. Med. Rep.* **11**, 1566–1572 (2015).
29. S. Horvath, DNA methylation age of human tissues and cell types. *Genome Biol.* **14**, R115 (2013).
30. Y. Dor, H. Cedar, Principles of DNA methylation and their implications for biology and medicine. *Lancet* **392**, 777–786 (2018).
31. S. Horvath *et al*., Obesity accelerates epigenetic aging of human liver. *Proc. Natl. Acad. Sci. U.S.A.* **111**, 15538–15543 (2014).
32. J. S. Johansen *et al*., Serum YKL-40 is increased in patients with hepatic fibrosis. *J. Hepatol.* **32**, 911–920 (2000).
33. T. B. Kelleher *et al*., Prediction of hepatic fibrosis in HIV/HCV co-infected patients using serum fibrosis markers: The SHASTA index. *J. Hepatol.* **43**, 78–84 (2005).
34. P. Y. Bochud *et al*.; Swiss Hepatitis C Cohort Study Group, Genotype 3 is associated with accelerated fibrosis progression in chronic hepatitis C. *J. Hepatol.* **51**, 655–666 (2009).
35. M. Rizzetto, Hepatitis D: Thirty years after. *J. Hepatol.* **50**, 1043–1050 (2009).
36. T. Kisseleva, The origin of fibrogenic myofibroblasts in fibrotic liver. *Hepatology* **65**, 1039–1043 (2017).
37. Y. A. Lee, M. C. Wallace, S. L. Friedman, Pathobiology of liver fibrosis: A translational success story. *Gut* **64**, 830–841 (2015).
38. S. L. Friedman, Mechanisms of hepatic fibrogenesis. *Gastroenterology* **134**, 1655–1669 (2008).
39. J. E. Puche, Y. Saiman, S. L. Friedman, Hepatic stellate cells and liver fibrosis. *Compr. Physiol.* **3**, 1473–1492 (2013).
40. M. Kaviratne *et al*., IL-13 activates a mechanism of tissue fibrosis that is completely TGF-beta independent. *J. Immunol.* **173**, 4020–4029 (2004).
41. S. R. Ignat, S. Dinescu, A. Hermenean, M. Costache, Cellular interplay as a consequence of inflammatory signals leading to liver fibrosis development. *Cells* **9**, 461 (2020).
42. M. Melis *et al*., Viral expression and molecular profiling in liver tissue versus microdissected hepatocytes in hepatitis B virus-associated hepatocellular carcinoma. *J. Transl. Med.* **12**, 230 (2014).
43. G. Diaz *et al*., Molecular signature and mechanisms of hepatitis D virus-associated hepatocellular carcinoma. *Mol. Cancer Res.* **16**, 1406–1419 (2018).
44. D. Harouaka *et al*., Diminished viral replication and compartmentalization of hepatitis C virus in hepatocellular carcinoma tissue. *Proc. Natl. Acad. Sci. U.S.A.* **113**, 1375–1380 (2016).
45. K. Ishak *et al*., Histological grading and staging of chronic hepatitis. *J. Hepatol.* **22**, 696–699 (1995).
46. P. Farci *et al*., B cell gene signature with massive intrahepatic production of antibodies to hepatitis B core antigen in hepatitis B virus-associated acute liver failure. *Proc. Natl. Acad. Sci. U.S.A.* **107**, 8766–8771 (2010).
47. E. Wang, L. D. Miller, G. A. Ohnmacht, E. T. Liu, F. M. Marincola, High-fidelity mRNA amplification for gene profiling. *Nat. Biotechnol.* **18**, 457–459 (2000).
48. R. Simon *et al*., Analysis of gene expression data using BRB-ArrayTools. *Cancer Inform.* **3**, 11–17 (2007).
49. B. Efron, R. Tibshirani, On testing the significance of sets of genes. *Ann. Appl. Stat.* **1**, 107–129 (2007).